FAST DYNAMIC FORCE COMPUTATION FOR ELECTROSTATIC AND ELECTROMAGNETIC CONDUCTORS

A Thesis

by

PRABHAVATHI KOTEESWARAN

Submitted to the Office of Graduate Studies of
Texas A&M University
in partial fulfillment of the requirements for the degree of

MASTER OF SCIENCE

December 2004

Major Subject: Computer Engineering

FAST DYNAMIC FORCE COMPUTATION FOR ELECTROSTATIC AND ELECTROMAGNETIC CONDUCTORS

A Thesis

by

PRABHAVATHI KOTEESWARAN

Submitted to Texas A&M University
in partial fulfillment of the requirements
for the degree of

MASTER OF SCIENCE

Approved as to style and content by:

Weiping Shi (Chair of Committee)	
Duncan M. H. Walker (Member)	Jiang Hu (Member)
Takis Zourntos (Member)	Chanan Singh (Head of Department)

December 2004

Major Subject: Computer Engineering

ABSTRACT

Fast Dynamic Force Computation for Electrostatic and
Electromagnetic Conductors. (December 2004)
Prabhavathi Koteeswaran, B.E., Anna University, Chennai, India
Chair of Advisory Committee: Dr.Weiping Shi

This thesis presents an improved method for dynamic force computation applicable to both electrostatic and electromagnetic conductors with complex 3D geometries. During the transient simulation of electrostatic actuated MEMS, the positions of the conductors as well as the potential applied to the conductors may change, necessitating recalculation of electrostatic forces at each time step of computation. Similarly, during the simulation of electromagnetic actuated MEMS, the current re-distribution in the conductors requires recalculation of electromagnetic forces at each time step. In this thesis, a simple method based on the principles of fast multipole algorithm is explored to effectively recalculate the potential coefficients to compute the surface charges and thereby forces during transient simulation of electrostatic conductors. The proposed method improves the speed of electrostatic force computation by 15 - 60% at each time step, depending on the displacement, with an error less than 3%. Electromagnetic forces are also computed by the same method. In addition, an efficient method is also presented for electrostatic analysis of dummy metal filled interconnects.

ACKNOWLEDGMENTS

I would like to express my sincere appreciation to Dr.Weiping Shi, whose guidance and support has made this research successful. I would also like to thank my family and friends for their encouragement and support.

TABLE OF CONTENTS

CHAPTER Page

LIST OF TABLES

LIST OF FIGURES

FIGURE Page

FIGURE Page

CHAPTER I

INTRODUCTION

Electrostatic and electromagnetic interactions form the fundamental basis for determining the design, dynamics and function of a variety of applications including MEMS actuators [1][2], bio-molecular simulations [3] and VLSI interconnects. Efficient functioning of the designed device, when it is embedded in a complete system is determined by accurate dynamical models that permit rapid simulation of system performance under a wide variety of inputs and scenarios. Typical simulations involve complex 3D geometries and various boundary conditions. These interactions cannot be determined statically. Dynamic simulation involves the determination of electrostatic or electromagnetic interactions at each discrete time interval. Hence efficient and accurate simulation tools are required for calculation of electrostatic and electromagnetic forces.

A. Electrostatic Conductors

When a voltage is applied between two conductors, electrostatic charges are induced on the surface of the conductors; the charges on the surface of one conductor exert forces on the other conductor. These forces act normal to the surface of the conductors and cause a deformation of the conductors. When the conductor deforms, the charges redistribute on the surface of the conductors, thereby changing the resultant forces. This process continues until an equilibrium is reached. This is the fundamental principle behind the functioning of electrostatic MEMS devices such as actuators and sensors [4].

The journal model is *IEEE Transactions on Automatic Control.*

Computational analysis of such devices involves an electrostatic analysis to compute the electrostatic forces acting on the conductors and a mechanical analysis to compute the deformation of the conductors. Electrostatic simulation is performed on the deformed position of the conductors, which involves re-discretization and re-computation of the electrostatic interactions at each time step during the analysis.

B. Electromagnetic Conductors

Electromagnetic interactions gain importance in high performance and high power applications because the magnitude of electrostatic forces is limited by the applied voltage. A current carrying conductor produces a magnetic field around the conductor. The magnetic field causes forces to act on moving charges which constitute current in the conductors. When the conductor deforms, the magnetic field produced by the conductor varies, thereby changing the resultant forces. This is the fundamental principle behind the functioning of electromagnetic MEMS devices [2]. Computational analysis of these devices involve an electromagnetic analysis to compute the electromagnetic forces acting on the conductors and a mechanical analysis to compute the deformation of the conductors.

C. Existing Work and Presented Work

For small geometries, simulation of MEMS devices can be done by creating reduced order models. However, for geometrically complex 3D conductors, developing models is a cumbersome task [5]. Efficient and accurate analysis of complex 3D conductors requires numerical methods to compute electrostatic forces at each computation step.

Efficient recomputation of surface forces on the deformed conductors during successive iterative steps is the main focus of this thesis. The motivation behind

this work is that, since electrostatic and electromagnetic analysis involve an iterative procedure, even a small reduction in the simulation of conductors at each time step would contribute significantly to the performance of static and dynamic simulation of these devices.

Wang [6] presented a dipole approach to compute electrostatic geometric sensitivities. They show that computing the charge distribution due to geometric perturbations is equivalent to obtaining charge distributions for linearly varying dipole distribution. However, the dipole approach can be applied to only linear geometric sensitivities. Also, for nearby panels, the predicted and the actual potential changes do not match for large perturbations.

Li [1] presented a Lagrangian approach to map the boundary integral equations of the deformed configuration onto the undeformed configuration. They reformulate the quantities in the deformed configuration by expressing the corresponding initial configuration and the displacement by a Lagrangian description, while our method effectively recomputes the integral equations of the deformed configuration by a closed form expression derived by Taylor's series expansion. Their method focuses on effectively reformulating the problem for complex 3D geometries, whereas the proposed method focuses on effectively computing the reformulated problem. The proposed method can be thus combined with the Lagrangian approach to reduce the computational complexity of complex 3D geometries.

In this thesis, an improved method is presented for dynamic force computation which is applicable to both electrostatic and electromagnetic conductors with complex 3D geometries. A simple method based on the principles of fast multipole method (FMM) is explored to effectively recalculate the force using the FMM data structure for the previous time step. The proposed method improves the speed of electrostatic force computation by 15% to 60%, depending on the displacement, with the error less

than 3%. Since electromagnetic forces can also be computed by BEM methods, this method can be easily extended.

Another important problem where effective electrostatic analysis is necessary is in the case of dummy filled interconnects. Chemical-Mechanical Planarization (CMP) and other manufacturing steps in very deep sub-micron VLSI have varying effects on device and interconnect features depending on local characteristics of the layout [7][8]. In order to improve the manufacturability and performance predictability, foundry rules require insertion of dummy metal fills into the layout to make it uniform with respect to prescribed density criteria. Improvements in uniformity at the process level must be carefully checked against design/electrical concerns of any added interconnect capacitance resulting from dummy metal fills. An efficient method for the electrostatic analysis of dummy conductor fills has been discussed.

Chapter II explains the basic principles of reducing computation time in fast force algorithms. In Chapter III, electrostatic analysis is explained in detail and performance and accuracy is analyzed for various force algorithms. Chapter IV describes electromagnetic analysis in detail. Chapter V presents the new Translation Method for effectively recalculating forces by employing the FMM data structure of the previous step. Electrostatic analysis of dummy metal filled interconnects is discussed in Chapter VI.

CHAPTER II

FORCE CALCULATION - N BODY ALGORITHMS

The force calculation problem is classified as an n-body problem. In the n-body problem, each of the n particles exert a force on each of the $n-1$ particles resulting in $O(n^2)$ interactions. In this chapter, some of the principles in reducing the complexity adopted by popular algorithms have been discussed. Efficient algorithms have been developed for N-body simulation of particles interacting in a gravitational field by Appel [9], Barnes and Hut [10] and by Greengard [11]. Electrostatic, electromagnetic and gravitational forces share some common properties - they all follow the same inverse square law with respect to the distance between the elements. Also, the superposition principle by which the total force can be expressed as the sum of the contributions of all other elements, applies to the calculation of all three forces. The similarity between the three forces permits the extension of the N-body algorithms for gravitational forces to the calculation of electrostatic and electromagnetic forces.

A. Appel's Hierarchical Algorithm

Appel introduced a hierarchical divide and conquer algorithm [9] for the simulation of particles interacting in a gravitational field. Initially, the complexity of the algorithm was estimated as $O(N \log N)$ by Appel [9], but was proven to be $O(N)$ by Esselink [12]. The basic idea behind reducing the complexity of the problem is the use of monopole approximation principles.

1. Monopole Approximation

In this approximation, the interaction produced by a cluster of particles is approximated by a single particle acting at the center of mass of the cluster, resulting in the

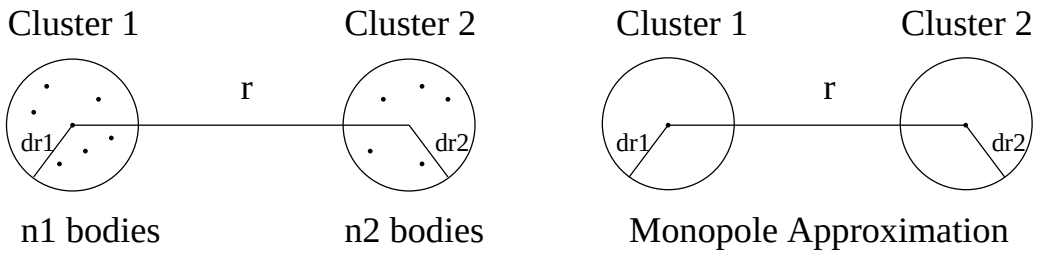

Fig. 1. Appel's monopole approximation

calculation of just one interaction instead of interactions caused by each of the particles present in the cluster. Consider two clusters of particles shown in Fig. 1, cluster 1 containing $n1$ bodies and cluster 2 containing $n2$ bodies. Total force computation on each particle due to all other particles can be done in 3 steps: computing all local interactions in cluster 1, computing all local interactions in cluster 2, and computing the interactions of each particle in cluster 1 with each particle in cluster 2. When the clusters are separated by a sufficient distance, the inter-cluster interactions can be attacked by monopole approximation technique. The interactions which satisfy $\frac{dr1}{r} < \delta$ and $\frac{dr2}{r} < \delta$, where δ is a fixed criterion for accuracy, can be approximated to that of a single pseudo-particle acting at the center of each cluster as shown in Fig. 1. All local interactions within a cluster are computed directly.

Error introduced by the monopole approximation is of order $\left(\frac{dr}{r}\right)^2$ where $dr = \max(dr1, dr2)$ indicating that the monopole approximation works very well for clusters separated by large distances.

B. Fast Multipole Method

FMM (Fast Multipole Method) [11][13] is an algorithm for rapid evaluation of potential and electrostatic fields due to the distribution of charges. Complexity of this algorithm is $O(N)$. Multipole and local expansions represent the key concepts behind

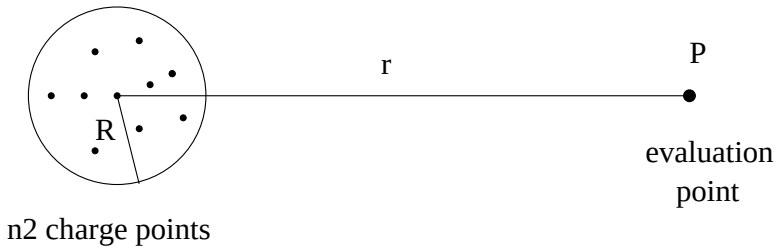

Fig. 2. Multipole expansion

reducing the complexity of the algorithm to $O(N)$.

1. Multipole Expansion

Multipole expansions describe the far field potential about the center of a cluster due to particles inside the cluster [11]. They exploit the fact that for $r >> R$, the electrostatic field can be computed in fewer operations by using approximations.

The field at any evaluation point P at a distance r as shown in Fig. 2 is not strongly influenced by the details of distribution of charges inside the circle of radius R [14]. The field at the evaluation point can be computed by replacing the $n2$ charge points by a single pseudo charge equal to the sum of charges located at the center of the cluster of charge points.

For $n1$ evaluation points separated by a distance of r from the cluster of charge points, computation of multipole coefficients requires $O(n1 + n2)$ operations - $n2$ operations to compute the equivalent charge acting at the center of the circle and $n1$ operations to calculate potentials at $n1$ evaluation points [14].

2. Local Expansion

Local expansions describe the electrostatic field about the center of a cluster due to all particles outside the cluster and its nearest neighbors [11]. Since the charge points

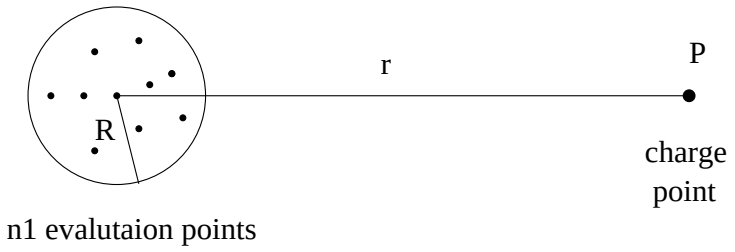

Fig. 3. Local expansion

are widely distributed and the evaluation points are clustered together, the evaluation points can be approximated at the center of the cluster of evaluation points.

For $n2$ charges separated by a distance r as shown in Fig. 3, computation of local coefficients requires $O(n1 + n2)$ operations - $n2$ operations to compute the electrostatic field at the center of the circle and $n1$ operations to transfer the potential at center to $n1$ evaluation points [14].

The computation error in using the multipole and local expansion depends on the distance of separation r of the clusters and the number of terms p used in the multipole expansion, i.e. $\left(\frac{r}{R}\right)^p$. Thereby, sufficiently separated clusters can be approximated by fewer orders of multipole and local expansion.

In the following chapters, application of these algorithms to reduce the computation of electrostatic and electromagnetic analysis will be discussed.

CHAPTER III

ELECTROSTATIC ANALYSIS

A. Electric Field and Forces

Electrostatic fields and forces are characterized by the Coulomb's law of electrostatic interactions. The electrostatic field can be described as the negative of the gradient of potential. If a point charge is located at a point $X_0 = (x_0, y_0, z_0)$, then for any point $X = (x, y, z)$ with $X \neq X_0$, the potential and electrostatic fields due to this charge can be described as

$$\phi_{X_0}(X) = \frac{1}{4\pi\epsilon_0 \parallel X - X_0 \parallel} \tag{3.1}$$

$$E_{X_0}(X) = -\nabla\phi_{X_0} = \frac{(X - X_0)}{4\pi\epsilon_0 \parallel X - X_0 \parallel^3} \tag{3.2}$$

The force F exerted on a charge q in an electric field E is defined as

$$F = qE \tag{3.3}$$

B. Computation of Surface Charge and Electrostatic Fields

1. Surface Charges

Given the conductor potentials, the surface charges can be solved using an equivalent free space formulation where the conductor dielectric interface is replaced by a charge layer of density [15]. The charge layer satisfies the following first-kind integral

equation.

$$\psi(x) = \int_S \sigma(x') \frac{1}{4\pi\epsilon_0 \parallel x - x' \parallel} da' \tag{3.4}$$

where $\psi(x)$ is the known conductor surface potential, da' is the incremental conductor surface area, $x, x' \in R^3$, $x' \in da'$ and $\parallel x - x' \parallel$ is the euclidean distance between x and x'.

Galerkin scheme is usually employed to numerically solve (3.4) for σ. In this approach, the surface of the conductors is divided into n small panels; and a charge q_i is assumed to be uniformly distributed on each panel A_i. For each panel, an equation is written relating the known potential on A_i denoted by v_i, to the sum of contribution of potential from charges on all n panels $A_1, A_2, A_3....A_n$. This results in a dense linear system

$$Pq = v \tag{3.5}$$

where $q \in R^n$ is the vector of panel charges, $v \in R^n$ is the vector of known panel potentials, $P \in R^{n \times n}$ is the potential coefficient matrix. Each entry of P is defined as

$$P_{ij} = \frac{1}{area(A_i)} \int_{A_i} \frac{1}{area(A_j)} \int_{A_j} \frac{1}{4\pi\epsilon_0 \parallel x - x' \parallel} da_i da_j \tag{3.6}$$

for panels A_i and A_j.

The integration in (3.6) is computed by numerical methods. The panel charges are computed by solving the linear system (3.5). Since the matrix P is dense and large, iterative methods such as GMRES are used and accelerated by fast multipole method.

2. Electrostatic Field

Employing the relation between the electrostatic and potential field from (3.2), electrostatic field coefficient in direction k for two panels A_i and A_j is given as

$$(C_{ij})_k = \frac{1}{area(A_i)} \int_{A_i} \frac{1}{area(A_j)} \int_{A_j} \frac{(x - x')_k}{4\pi\epsilon_0 \| \ x - x' \ \|^3} da_i da_j \tag{3.7}$$

where $(x - x')_k$ represents the k^{th} component of the vector $(x - x')$.

The k^{th} component of electrostatic field vector $(E_i)_k$ for a panel A_i is computed as the product of corresponding component of field coefficient $(C_{ij})_k$ and charge q_j at panel A_j, for all A_j that has interaction with A_i.

$$(E_i)_k = \sum_{\substack{j=all\ links, \\ j \neq i}} (C_{ij})_k . \, q_j \tag{3.8}$$

C. Analysis and Discussion of Force Algorithms

The hierarchical refinement algorithm [15] has been adapted for the calculation of electrostatic fields because of its simplicity, increased storage efficiency and performance. The hierarchical refinement algorithm is based on Appel's monopole algorithm and is accelerated by FMM method. It can be therefore viewed as $zero^{th}$ -order FMM. The kernel independent property of this algorithm further helps us to easily extend the algorithm for the calculation of electrostatic fields.

Electrostatic analysis is performed for a typical element of MEMS electrostatic combdrive as shown in Fig. 4. Their dimensions are as explained below:

$l_f, l_m \rightarrow$ length of the fixed and moving finger respectively.

$w_f, w_m \rightarrow$ width of the fixed and moving finger respectively.

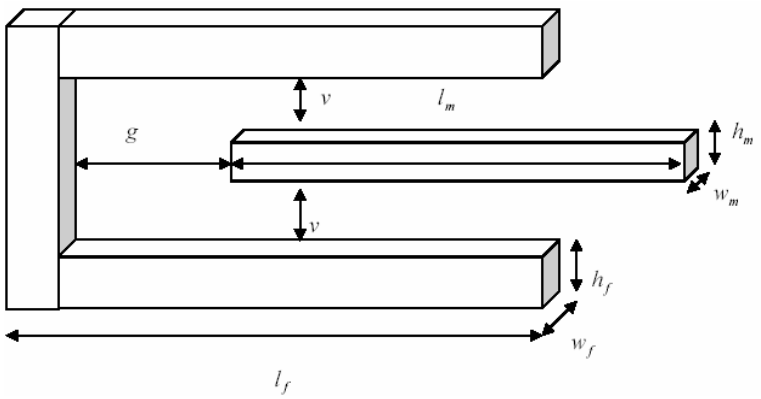

Fig. 4. Combdrive example

$h_f, h_m \rightarrow$ height of the fixed and moving finger respectively

$g \rightarrow$ horizontal gap between the fixed and moving finger

$v \rightarrow$ vertical gap between the fixed and moving finger

As the gap g between the fixed and moving fingers decreases, the electrostatic interactions between the fingers increase. Thereby, performing electrostatic analysis on a single combdrive for various values of gap would give a good estimate of the validity of the algorithm for a wide range of interactions.

The experiments were carried out for the following values

$l_f = l_m = 40\mu m$, $w_f = w_m = 4\mu m$, $h_f = h_m = 2\mu m$, $v = 3\mu m$

The accuracy of the algorithm is calculated by comparing with the direct pairwise force F_{dir} given by the Coulomb's law. Error estimation is given by the relative error of resultant force vectors, $err = \frac{F_{dir} - F_{alg}}{F_{dir}}$. The timing performances are given based on the execution time taken on a SUN SOLARIS machine.

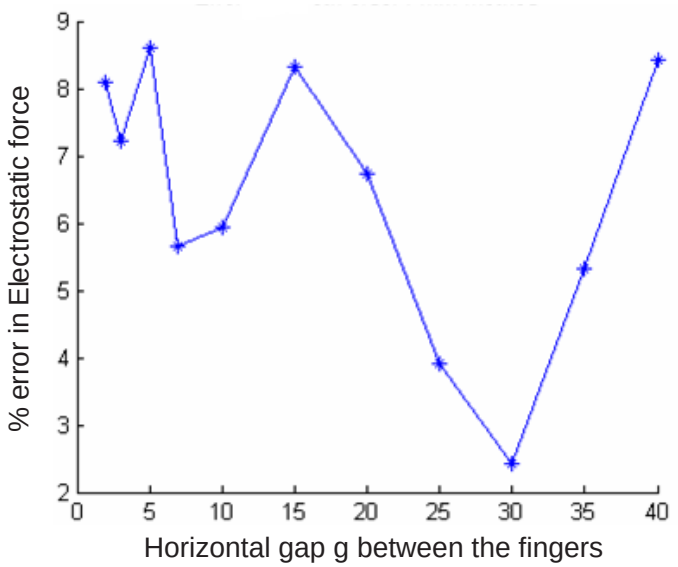

Fig. 5. Error by $zero^{th}$ order FMM

1. $Zero^{th}$ order FMM

As shown in Fig. 5, the error in the force calculation by zeroth order FMM method ranges from 2.43% to 8.08%.

As seen in Fig. 6, the error in potential/ capacitance problem is much less than the error in field/ force problem. This is because the error produced by the hierarchical algorithm is dependent of the discretization of panels. In order to use zeroth order FMM for field problem, further fine discretization of panels based on $\frac{r_s}{r^2}$ is required. Since further discretization of conductors would be very expensive for both the capacitance and the force problem, other reasons for this unacceptable error obtained and methods for improving the error are analyzed in the next section.

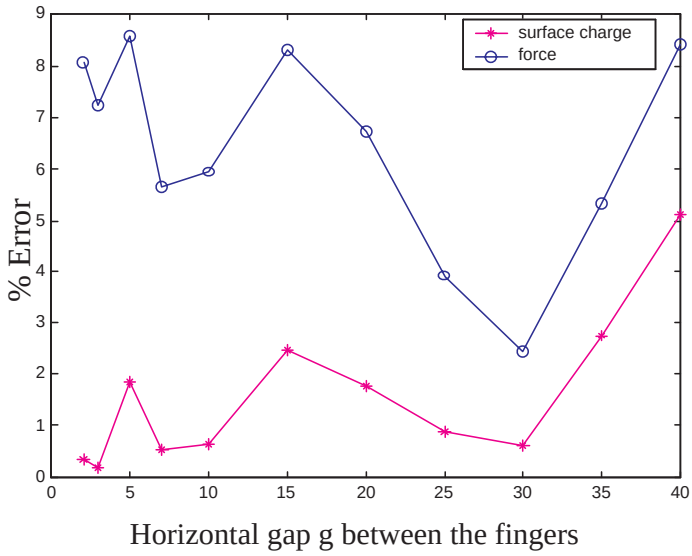

Fig. 6. Error comparison of force with surface charge

2. Error Analysis and Improvement

a. Numerical Integration

One of the reasons for the error could be the approximation of the electrostatic field coefficient matrix C during numerical integration. This type of error could be improved by increasing the number of interactions considered for field calculation between every two panels.

The error obtained by improving the integration is recorded in Table I. Fig. 7 shows the error obtained for various levels of interactions between the panels. Improving the numerical integration improves the error only for certain cases and deteriorates for certain other cases and also results in increased computation time. The error limits obtained are still much higher than acceptable limits.

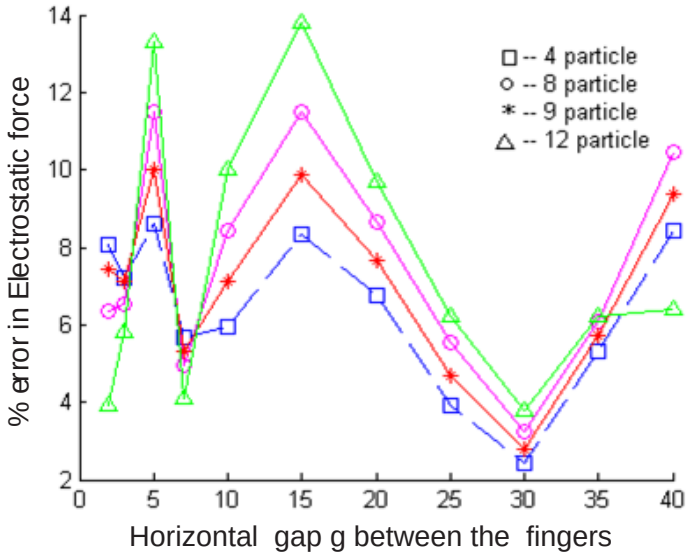

Fig. 7. Error – Improving numerical integration

Table I. Results – Improving numerical integration

Number of particles in each panel	Total number of interactions	Average Computation Time (s)	Error Range
4	16	0.0836	2.43% – 8.59%
8	64	0.352	3.26% – 11.5%
9	81	0.355	2.77% – 10.33%
12	144	3.6	3.8% – 13.8%

b. Unbalanced Charge Distributions

Other sources of error could include the truncation of the multipole expansion to zeroth order and the assumption of uniform charge density on large panels. The relation between charge distribution and error in potential calculation has been explained in [16][17]. Errors in the calculation of electrostatic field can be estimated on similar grounds.

When a panel A is subdivided into two panels A_1 and A_2 , the error in electrostatic field at $x \in A$ by considering it as a single panel A, due to charges in A_1 and A_2 with uniform charge distribution σ_1 and σ_2 respectively, can be described as

$$Error = \int_A \frac{\sigma_1+\sigma_2}{2}\frac{1}{4\pi\epsilon_0 \parallel x-x' \parallel^2}da' - \int_{A_1}\frac{\sigma_1}{4\pi\epsilon_0 \parallel x-x' \parallel^2}da' - \int_{A_2}\frac{\sigma_2}{4\pi\epsilon_0 \parallel x-x' \parallel^2}da'$$

Assuming without loss of generality that $\sigma_2 \geq \sigma_1$,

$$= \frac{1}{4\pi\epsilon_0}\frac{\sigma_2-\sigma_1}{2}\left[\int_{A_1}\frac{1}{\parallel x-x' \parallel^2}da' - \int_{A_2}\frac{1}{\parallel x-x' \parallel^2}da'\right]$$

$$\leq \frac{1}{4\pi\epsilon_0}\frac{\sigma_2-\sigma_1}{2}\left[\int_{A_1}\left(\frac{1}{\parallel x-x' \parallel^2} - \frac{1}{\parallel x-x'+r_s \parallel^2}\right)da'\right]$$

where r_s is the minimum radius of sphere enclosing the panel A.

$$\leq \frac{1}{4\pi\epsilon_0}\frac{\sigma_2-\sigma_1}{2}\left[\int_{A_1}\frac{r_s^2+2rr_s}{\parallel x-x' \parallel^2 \parallel x-x'+r_s \parallel^2}da'\right]$$

$$\leq \frac{1}{4\pi\epsilon_0}\frac{q_2-q_1}{2}\left[\frac{r_s^2}{r^2}C_{12} + \frac{2r_s}{r^2}P_{12}\right]$$

$$\leq \frac{q_2-q_1}{4\pi\epsilon_0}\left[\frac{r_s}{r^2}P_{12}\right]$$

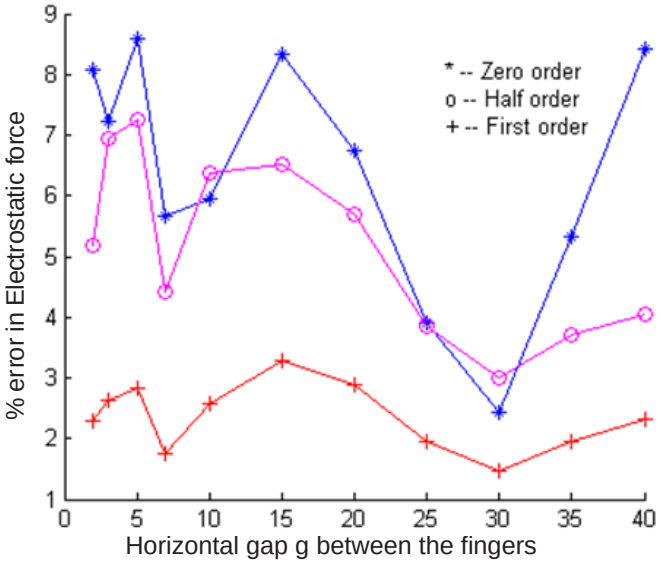

Fig. 8. Error – Higher order FMM

It can be seen from above that the error in the electrostatic field coefficient depends on the difference in charge distribution of the two sub-panels. Thereby, panels containing non-uniform charge distributions could lead to increased errors.

A variable order multipole scheme was presented in [16] to reduce errors caused by non-uniform charge distributions. The order of multipole expansion can be increased by going down the hierarchical tree. Going down one level is equivalent to half order multipole and first order multipole can be obtained by going down two levels. The error obtained by applying half and first order multipole is shown in Fig. 8 and the performance of this method is given in Table II.

It is observed that the error obtained by using first order multipole method is well within acceptable limits, although the average computation time increases by 33% compared to zeroth order. The results are shown for applying first order multipole and half order multipole to all the panels. Applying variable order multipole method, i.e, calculating increased orders of multipole only for those panels with large non-uniform

Table II. Results – Higher order FMM

Multipole order	Average Computation Time (s)	Error Range
0	0.0836	$2.43\% - 8.59\%$
$\frac{1}{2}$	0.166	$3\% - 6.53\%$
1	1.119	$1.48\% - 3.29\%$

charge distributions, the performance can be further improved.

c. Electric Field Properties

One of the important properties of the electric field flux, given by Gauss's law is its independence to the radius of the enclosing surface for any point charge enclosed by the surface. This special property of the electric field further simplifies the calculation, improves the performance and resulting errors. The integral form of the Gauss's law is given as

$$\Phi = \int_{Surface} E.\, ds = \frac{q}{\epsilon_0} \tag{3.9}$$

In other words, the field acting on a surface is proportional to the charge present on the surface and is independent of its distance from the field producing charges. Also, the electric field inside a closed surface is zero and all the electric field lines produced are perpendicular to the surface. Thereby, the electrostatic field $(E_j)_\perp$ for a panel A_j

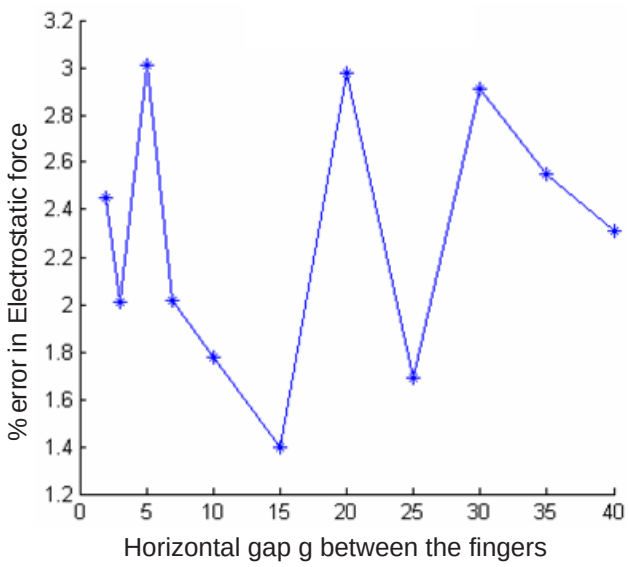

Fig. 9. Error – Gauss's law

of area a_j in the direction perpendicular to the surface of the panel is computed as the total charge on the surface of the panel divided by the permittivity of the medium and the area of the panel.

$$(E_j)_\perp = \frac{q_j}{2\epsilon_0 a_j} \tag{3.10}$$

The error obtained by this method ranges from 1.4% to 3% as shown in Fig. 9. The field has to be computed only in one direction for each panel, and the force can be computed directly at the leaf panels without any traversals of the tree, thereby improving the performance by a higher degree compared to the other algorithms.

CHAPTER IV

ELECTROMAGNETIC ANALYSIS

A. Computation of Branch Currents

Integral equation approaches for electromagnetic interactions are based on the magnetoquasistatic assumption that the contribution of displacement current $\epsilon\omega E$ to the magnetic field is negligible. With the above assumption, the current through a long thin conductor can be assumed to flow parallel to its surface as if there is no charge accumulation on the surface [18]. For long conductors, the conductors can be discretized into a number of filaments of rectangular cross section, inside each of which the current can be assumed to flow parallel to its length. The interconnection of the current filaments can be represented by a graph consisting of n nodes and b branches, with each branch representing a filament and each node representing the connection between the filaments. Thus a system of b equations can be generated for the conductors as follows

$$\frac{l_i}{\sigma a_i} I_i + j\omega \sum_{j=1}^{b} \left(\frac{\mu}{4\pi a_i a_j} \int_{V_i} \int_{V_j'} \frac{l_i \cdot l_j}{\parallel r - r' \parallel} dV' dV \right) I_j = \frac{1}{a_i} \int_{a_i} (\Phi_A - \Phi_B) dA \qquad (4.1)$$

where l_i is the unit length vector of the filament i, a_i is the cross section of filament i, Φ_A and Φ_B are the scalar potentials on the filament end faces, and V_i and V_j' are the volumes of filaments i and j respectively. In matrix form (4.1) can be written as

$$ZI_b = V_b \qquad (4.2)$$

where $Z = R + j\omega L \in C^{b \times b}$ is the branch impedance matrix that consists of a diagonal matrix $R \in R^{b \times b}$ of filament DC resistances and a dense matrix $L_{ij} \in R^{b \times b}$of partial

inductances, $V_b \in C^b$ is the vector of branch voltages and $I_b \in C^b$ is the vector of branch/filament currents.

Faster convergence of iterative solvers can be obtained by using mesh formulation for the filaments[18]. The mesh currents I_m and source voltages V_s are related to the branch currents I_b and voltages V_b as follows

$$MV_b = V_s \quad ; \quad M^t I_m = I_b \tag{4.3}$$

where $M \in R^{m \times b}$ is the mesh matrix. Combining (4.3) and (4.2) gives

$$MZM^t I_m = V_s \tag{4.4}$$

The equation (4.4) is usually solved by iterative methods like conjugate residual GMRES method and is accelerated by hierarchical multipole algorithm similar to electrostatic analysis [18].

B. Computation of Magnetic Field and Forces

The Biot Savart's Law relates the magnetic flux density to the current. The electromagnetic field produced by an element of length dl_1 of filament 1 in the direction of current I_1 flowing in the filament at a point specified by a location vector r, can be described as

$$dB = I_1 \, dl_1 \times \frac{\mu_0}{4\pi} \frac{r - r_1}{\| \, r - r_1 \, \|^3} \tag{4.5}$$

where r_1 is the location vector of length dl_1.

Total magnetic force acting on a filament is the vector sum of the electromagnetic forces exerted by all other filaments. The force F_2 exerted on filament 2 by

filament 1 can be expressed as

$$F_2 = \oint I_2 \, dl_2 \times B_1 \tag{4.6}$$

where B_1 is the magnetic flux density due to filament 1 at the position where filament 2 is located, I_2 is the current flowing through filament 2 and integration is performed over the loop of current flow through filament 2. Further, (4.6) can be combined with (4.2) and simplified as

$$F_2 = -\frac{\mu_0}{4\pi} \, I_1 \, I_2 \oint_2 \oint_1 \frac{(dl_1 \cdot dl_2)(r_2 - r_1)}{\parallel r_2 - r_1 \parallel^3} \tag{4.7}$$

C. Electrostatic Analogy

The magnetic field and electrostatic field can be related in the same way as the vector potential and scalar potential described in [18].Force exerted by one current loop on another can be obtained by applying mesh transformation on filament forces. The force exerted on a filament i by all other filaments can be expressed as

$$\begin{aligned} F_i &= -I_i \sum_{\substack{j=1 \\ j \neq i}}^{b} \left(\frac{\mu_0}{4\pi a_i a_j} \int_{V_i} \int_{V_j'} \frac{(l_i \cdot l_j)(r - r')}{\parallel r - r' \parallel^3} dV' dV \right) I_j \\ &= -\frac{I_i}{a_i} \int_{V_i} C(r) \cdot l_i dV \end{aligned}$$

where

$$C(r) = \frac{\mu_0}{4\pi} \sum_{\substack{j=1 \\ j \neq i}}^{b} \left(\int_{V'_j} l_j \frac{(r - r')}{\parallel r - r' \parallel^3} dV' dV \right) \frac{I_j}{a_j} \tag{4.8}$$

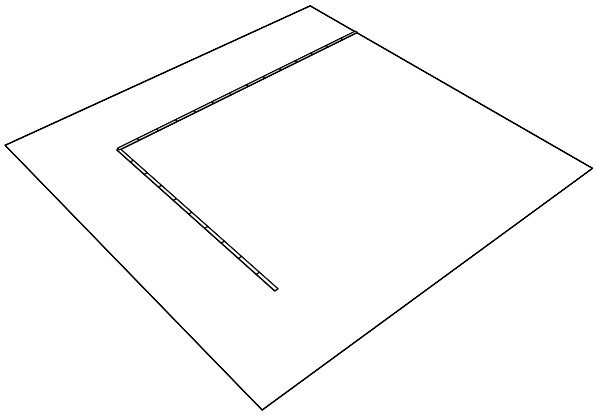

Fig. 10. Single filament over a ground plane

The vector components of $C(r)$ corresponding to the p^{th} component of l_j can be considered as the field vector $E_p(r)$ given by

$$E_p(r) = \frac{\mu_0}{4\pi} \sum_{\substack{j=1 \\ j \neq i}}^{b} \left(\int_{V'_j} (l_j)_p \frac{(r - r')}{\| r - r' \|^3} dV' dV \right) \frac{I_j}{a_j} \tag{4.9}$$

which is similar to electrostatic field vector with $\frac{I_j}{a_j}(l_j)_p$ interpreted as the charge density due to filament j. Evaluation of these field vectors can be computed by FMM method explained in chapter III in $O(b)$ time for each direction of length vector.

D. Results

Fasthenry [18] code was modified to calculate the electromagnetic force exerted on the conductors. For the simple example of a filament over a ground plane as shown in Fig. 10, with two conductors, the forces were calculated by FMM method and compared with the direct pairwise force. The results of the force vector computed by fmm of order 2 are as shown in Table III.

Time taken to calculate Force – Direct Method – 35.07s

Time taken to calculate Force – FMM Method – 3.19s

Table III. Results – Error by FMM method

.

Direct Force	FMM force	%Error
$1.19448e^{-25}$	$1.19464e^{-25}$	-0.013
$8.66398e^{-26}$	$8.66505e^{-26}$	-0.012
$-9.45961e^{-30}$	$-9.45402e^{-30}$	0.059

CHAPTER V

NEW TRANSLATION METHOD

For any two panels, each panel containing n charges, n^2 interactions need to be recomputed to determine their new potential coefficient at a displaced position. Since the potential coefficient matrix P is a dense matrix, effectively re-computing P is the key to improving the performance of dynamic force computation.

A. Integral Equation Approach

Consider two panels A_i and A_j separated by a distance r as shown in Fig. 11. When panel A_i is displaced by a distance d, the new potential coefficient $P_{i'j}$ between the displaced panel $A_{i'}$ and the panel A_j is obtained from the integral equation approach as

$$P_{i'j} = \frac{1}{area(A_{i'})area(A_j)} \int_{A_{i'}} \int_{A_j} \frac{1}{r'} da_j da_{i'} \tag{5.1}$$

where $r' = \parallel x_{i'} - x_j \parallel$ with $x_{i'} \in A_{i'}$ and $x_j \in A_j$.

In this approach, integration has to be recomputed for all charges in A_j with all charges in $A_{i'}$. For n charges in each panel, computation time can be of order $O(n^2)$.

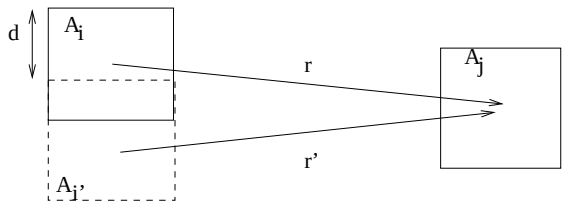

Fig. 11. Displaced panel

B. Translation Approach for $Zero^{th}$ Order FMM

The new potential coefficient can also be obtained by translating the original potential coefficient P_{ij} by the displacement d of panel A_i, for small displacements compared to their distance of separation r. FMM [11] employs this Translation principle from Taylor's expansion to reduce the computational complexity of force calculation. The new potential coefficient for a $zero^{th}$ order expansion can be obtained as shown below

$$\begin{aligned}
P_{i'j} &= \frac{1}{area(A_{i'})area(A_j)} \int_{A_{i'}} \int_{A_j} \frac{1}{r'} da_j da_{i'} \\
&= \frac{1}{area(A_i)area(A_j)} \int_{A_i} \int_{A_j} \left(\sum_{p=0}^{\infty} \frac{(-1)^p}{n!} . d^p . \frac{\partial^p}{\partial r^p} \left(\frac{1}{r} da_j da_i \right) \right) \\
&= \sum_{p=0}^{\infty} (-1)^p . d^p \left(\frac{1}{area(A_i)area(A_j)} \int_{A_i} \int_{A_j} \frac{1}{r^{p+1}} da_j da_i \right) \\
&= \sum_{p=0}^{\infty} (-1)^p . d^p . P_{ij}^{p+1}
\end{aligned}$$

where p is the number of terms in the expansion and can be truncated based on the required accuracy.

From Fig. 12, it can be observed that the potential coefficient obtained from the Translation Method converges for $p < 10$ for sufficiently separated panels. (i.e $\frac{d}{r} \leq 0.7$). Computing p terms by Translation Method is computationally less expensive than calculating n^2 interactions by integral equation approach, as is the usual method.

C. Translation Approach for Higher Order FMM

Higher order FMM is often necessary to obtain required accuracy for functions which are of order $\frac{1}{r^n}$ with $n > 1$. Examples may include electrostatic field and inductance calculations discussed in the earlier chapters. If higher order FMM were to be used,

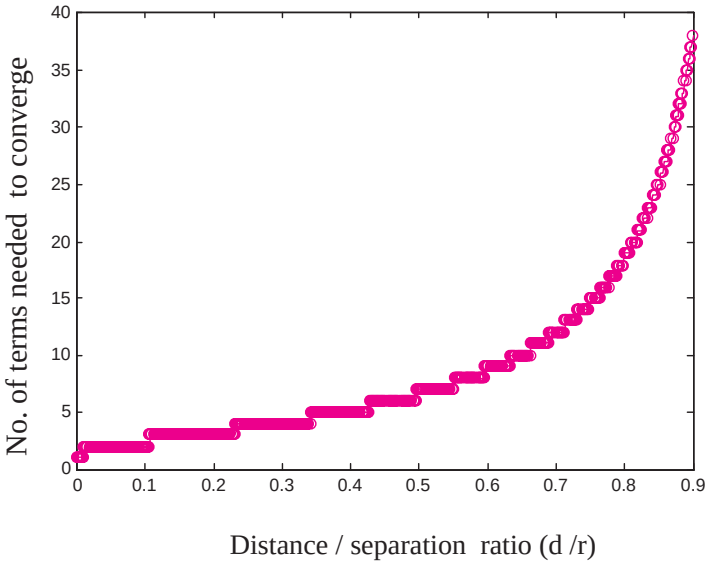

Fig. 12. Convergence of the Translation Method

the potential coefficient by the integral equation approach would be given as

$$P_{i'j} = \sum_{n=0}^{\infty} \sum_{m=-n}^{n} \int_{A_{i'}} \int_{A_j} \frac{Y_n^m(\theta', \phi')}{r'^{n+1}} \tag{5.2}$$

where $(A_{i'} - A_j) = (r', \theta', \phi')$ and $\frac{Y_n^m(\theta', \phi')}{r'^{n+1}}$ are spherical harmonics of degree $-n-1$ and order m with n being the number of terms needed for required accuracy.

For a small displacement of panel A_i given by $dA_i = (dr, d\theta, d\phi)$, the new potential coefficient $P_{i'j}$ can be expressed in terms of the original coefficient P_{ij} and the displacement dA_i using the First Addition Theorem given in [11] as

$$
\begin{aligned}
P_{i'j} &= \sum_{n=0}^{\infty}\sum_{m=-n}^{n}\int_{A_{i'}}\int_{A_j}\frac{Y_n^m(\theta',\phi')}{r'^{m+1}} \\
&= \sum_{n'=0}^{\infty}\sum_{m'=-n'}^{n'}\left(\int_{A_i}\int_{A_j}\sum_{n=0}^{\infty}\sum_{m=-n}^{n}\frac{J_m^{m'}.A_n^m.A_{n'}^{m'}}{A_{n+n'}^{m+m'}}.(dr)^n.Y_n^{-m}(d\theta,d\phi).\frac{Y_{n+n'}^{m+m'}(\theta,\phi)}{r^{n+n'+1}}\right) \\
&= \sum_{n'=0}^{\infty}\sum_{m'=-n'}^{n'}\sum_{n=0}^{\infty}\sum_{m=-n}^{n}\frac{J_m^{m'}.A_n^m.A_{n'}^{m'}}{A_{n+n'}^{m+m'}}.(dr)^n.Y_n^{-m}(d\theta,d\phi).\int_{A_i}\int_{A_j}\frac{Y_{n+n'}^{m+m'}(\theta,\phi)}{r^{n+n'+1}}
\end{aligned}
$$

where $A_n^m = \frac{(-1)^n}{\sqrt{(n-m)!(n+m)!}}$ and $J_m^{m'} = \begin{cases} (-1)^{min(|m'|,|m|)}, & \text{if } m.m' < 0. \\ 1 & \text{otherwise.} \end{cases}$

D. Results of Translation Method

The effectiveness of the Translation Method is shown by applying it to an example of combdrive for various displacements of the moving finger. The ratio of displacement of the moving finger to the distance between panels given by $\frac{d}{r}$ gives an account of the change in distance between the panels in the deformed position. For faraway panels, where the displacement d is less compared to the distance r between them, i.e. for small values of $\frac{d}{r}$, the Translation Method gives improved performance without much loss of accuracy.

In order to get a good estimate of the performance improvement, the experiments were carried out on a larger comb drive example with the following dimensions

$$l_f = l_m = 250\mu m,\ w_f = w_m = 5\mu m,\ h_f = h_m = 5\mu m,\ v = 3\mu m,\ g = 100\mu m$$

1. Displacement = 1.25 (0.5% of finger length)

It can be observed from Fig. 13 and Fig. 14 that applying the Translation principle

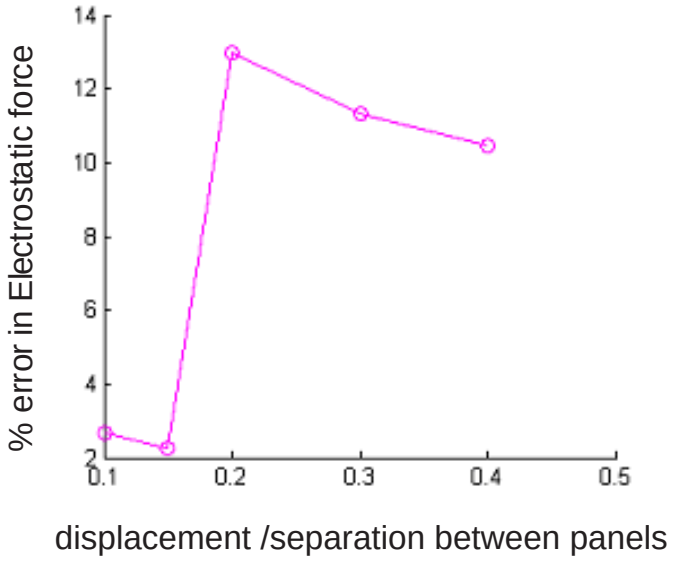

Fig. 13. Error – d=0.5% l_m

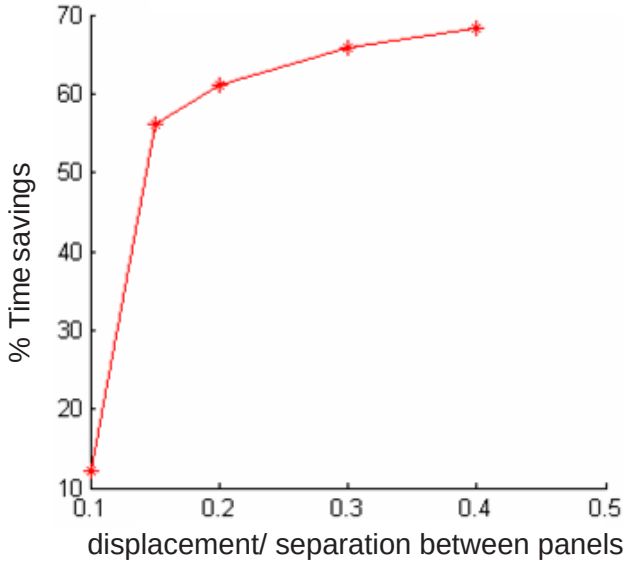

Fig. 14. Time savings – d=0.5% l_m

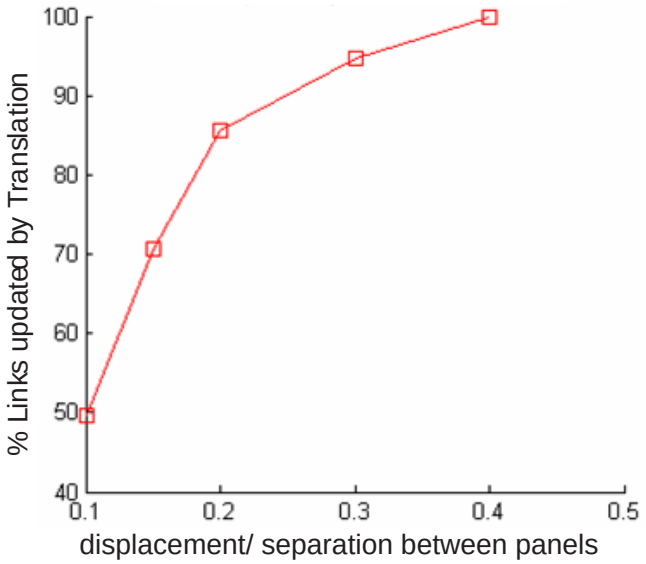

Fig. 15. Links updated – d=0.5% l_m

for well separated panels i.e. for panels satisfying $\frac{d}{r} \leq 0.15$, gives an improvement of 56.1% in performance with an error of only 2.26%. Fig. 15 gives an account of the number of links updated by the Translation Method for the given displacement. For the given $\frac{d}{r}$ ratio, around 70% of the links are updated by Translation.

2. Displacement = 12.5 (5% of finger length)

Fig. 16 and Fig. 17 show that applying the Translation principle for panels satisfying $\frac{d}{r} \leq 0.4$, gives an improvement of 9.76% in performance with an error of only 1.46%. It can be seen from Fig. 18 that around 19% of the links are updated by Translation for the given displacement for $\frac{d}{r} \leq 0.4$.

3. Displacement = 25 (10% of finger length)

It can be observed from Fig. 19 and Fig. 20 that applying the Translation principle for panels satisfying $\frac{d}{r} \leq 0.4$, give an improvement of 9.52% in performance with a

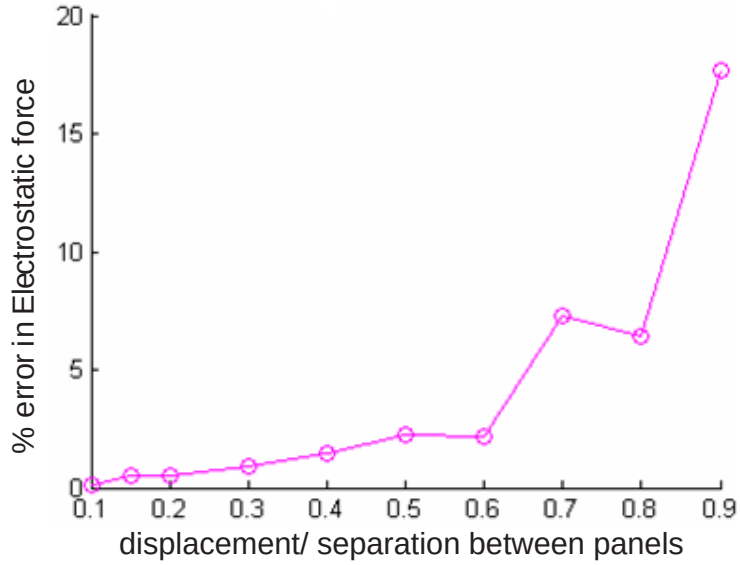

Fig. 16. Error – d=5% l_m

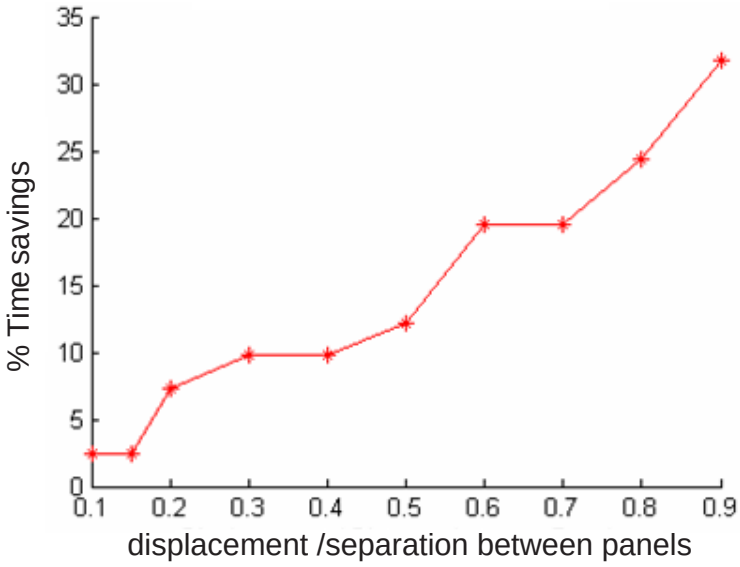

Fig. 17. Time savings – d=5% l_m

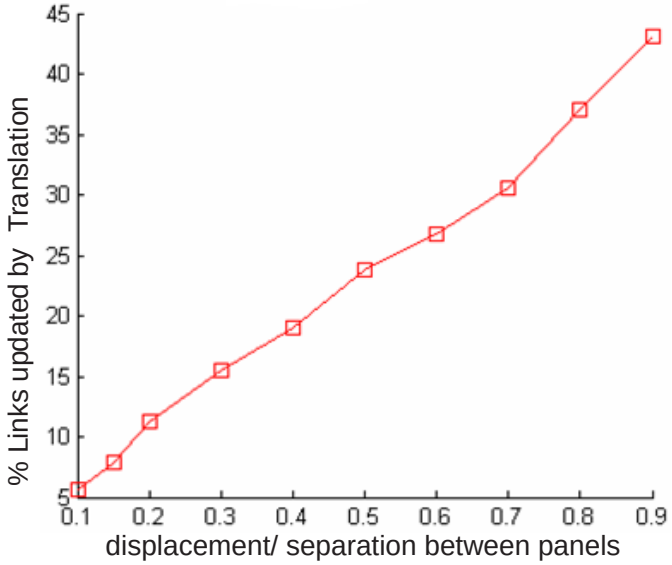

Fig. 18. Links updated – d=5% l_m

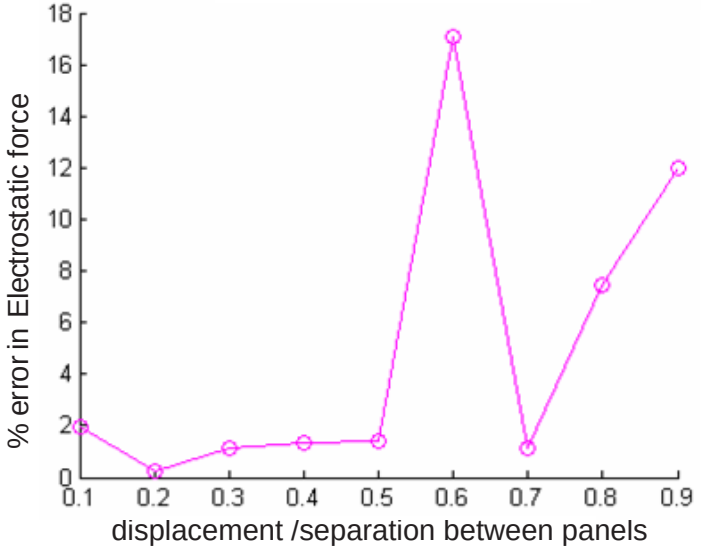

Fig. 19. Error – d=10% l_m

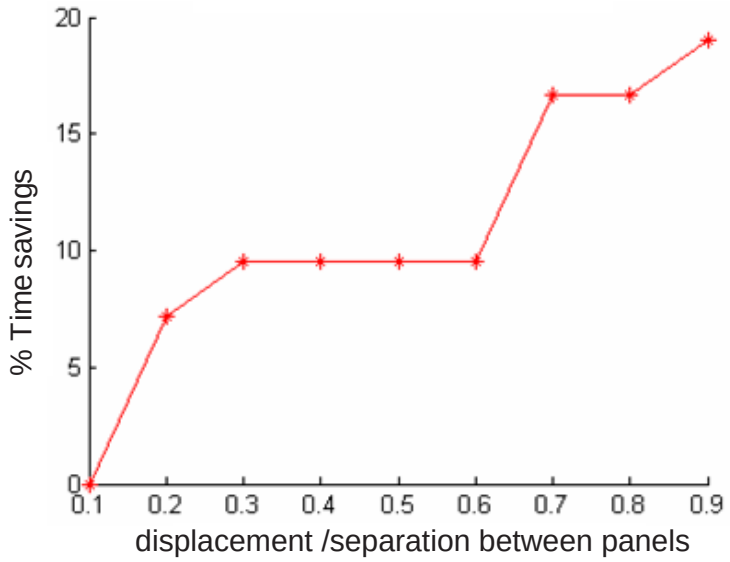

Fig. 20. Time savings – d=10% l_m

loss of only 1.43% in accuracy. For the given $\frac{d}{r}$ ratio, Fig. 21 shows that up to 13% of the links are updated by Translation.

As seen from the results, the Translation Method gives improved performance for sufficiently separated panels of the deformed conductor. It can be observed that, for smaller ranges of displacements, as is usually the case for static simulation, comparative improvement in performance can be achieved with a reasonable loss in accuracy. For larger displacements, which might occur during dynamic simulation, the performance is still improved by a factor of 10% during each iteration.

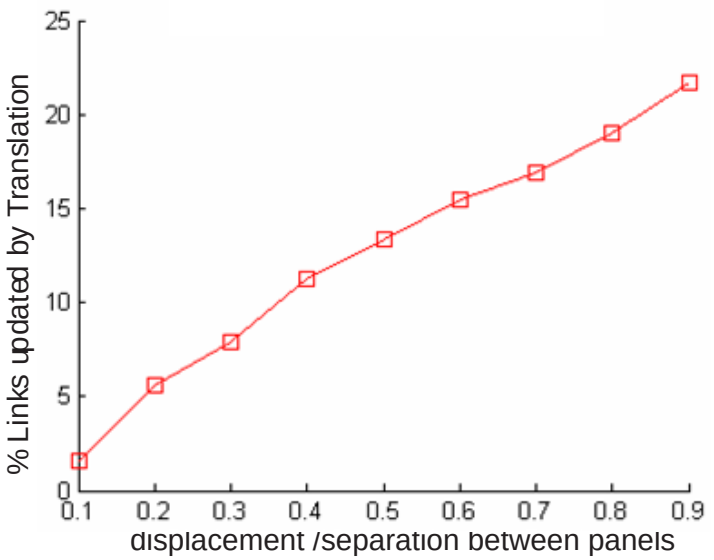

Fig. 21. Links updated – d=10% l_m

CHAPTER VI

ELECTROSTATIC ANALYSIS OF DUMMY FILLED INTERCONNECTS

Another important problem where effective electrostatic analysis is necessary is in the case of dummy filled interconnects. Chemical-Mechanical Planarization (CMP) and other manufacturing steps in very deep sub-micron VLSI have varying effects on device and interconnect features depending on local characteristics of the layout [7][8]. In order to improve the manufacturability and performance predictability, foundry rules require insertion of dummy metal fills into the layout as shown in Fig. 22 to make it uniform with respect to the prescribed density criteria. Improvements in uniformity at the process level must be carefully checked against design/electrical concerns of any added interconnect capacitance resulting from dummy metal fills. Since the number of dummy metals inserted is usually greater than the number of conductors involved, efficient methods for electrostatic analysis is of great importance.

Impacts of dummy metal fills on the performance include

1. Variation in inter-metal capacitance resulting from variation in line width
2. Errors due to proximity effects.
3. Changes in interconnect signal delay and crosstalks.

Overlap and fringe capacitance are not significantly affected by the insertion of small floating dummy features. The impact of dummy fills on lateral coupling capacitance between two active lines is of main concern. In order to minimize the effects of dummy metal fills on interconnect delay, it is essential to compute the capacitance and timing overheads before deciding on the size and pattern of dummy fills to be inserted. Fig. 23 shows various interconnect capacitances in the presence of dummy metal fills.

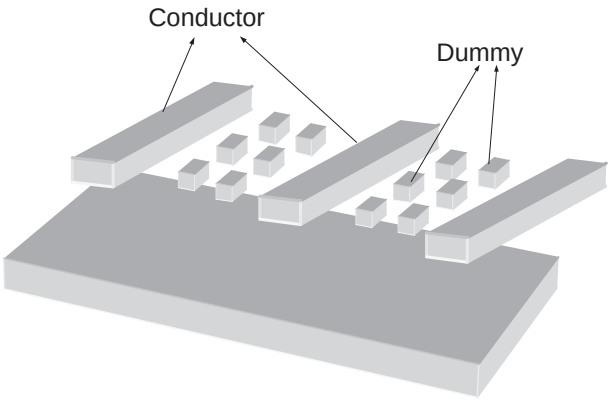

Fig. 22. Dummy metal fills

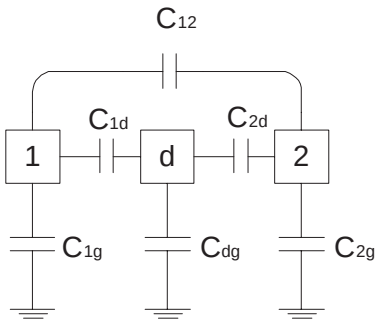

Fig. 23. Interconnect capacitances in the presence of dummy metal

Assuming there were m dummies and n conductors, two methods are discussed below for computing the capacitance overhead of dummies.

A. Method I

Consider the dummies as conductors and solve $(n + m)$ potential problems for the linear system $Pq = v$. The capacitance overhead on the conductors are then computed from the capacitance matrix. Fig. 23 shows the presence of a floating dummy d between conductor 1 and conductor 2. A floating dummy is a dummy metal which is not electrically connected. For the conductors shown in the Fig. 23, the capacitance overhead can be calculated from the capacitance matrix as

$$C_{1gnew} = C_{1g} + (C_{1d} \parallel C_{dg}) \tag{6.1}$$

$$C_{2gnew} = C_{2g} + (C_{2d} \parallel C_{dg}) \tag{6.2}$$

$$C_{12new} = C_{12} + (C_{1d} \parallel C_{2d}) \tag{6.3}$$

1. Advantages

1. Direct use of standard parasitic extraction tools to solve the linear systems.
2. Easier for grounded dummies since $C_{dg} = 0$ (since the dummy is grounded) $C_{dg} = C_{1g}$ (both are capacitances with respect to ground).

2. Disadvantages

1. Need to calculate C_{dg} for every dummy.
2. Number of dummies can be greater than the number of conductors
3. Need to perform $n + m$ linear system solves to calculate capacitance since we need to calculate ground capacitance of each dummy.

Since $m >> n$ in practical situations, this method would be computationally very expensive.

B. Method II

The electrical properties of the dummy conductors as explained below, can be used to effectively calculate their effect on the interconnect capacitance. Similar approach have been discussed in [19].

1. Induced charges on the dummy will lead to a potential on the corresponding dummy conductor
   $\sum_{dummy} Pq = v_{dummy}$
2. The sum of all charges induced on a dummy conductor is zero.
   $\sum_{dummy} q = 0$

The standard capacitance extraction tools cannot be used to solve the floating conductors since they are at unknown potentials. So the equations for the dummy are inserted into the capacitance solver by adding extra rows and columns in the linear system of equations $Pq = v$. For the conductors shown in Fig. 23, it can be done as shown below

$$\begin{bmatrix} p_{11} & p_{12} & p_{1d} & 0 \\ p_{21} & p_{22} & p_{2d} & 0 \\ p_{d1} & p_{d2} & p_{dd} & -1 \\ 0 & 0 & 1 & 0 \end{bmatrix} \begin{bmatrix} q_1 \\ q_2 \\ q_d \\ v_d \end{bmatrix} \begin{bmatrix} 1 \\ 0 \\ 0 \\ 0 \end{bmatrix} \tag{6.4}$$

It is to be noted that all the floating dummies are not at the same potential, therefore if we have m dummies, m rows and m columns have to added to the potential coefficient matrix and m additional rows are required in the charge and voltage vector.

Table IV. Results – Computation time of electrostatic analysis for dummy fills

No. of dummies	Method I CPU Time (s)	Method II CPU Time (s)	% Time savings
0	0.04	0.04	0
5	0.18	0.12	33.33
10	0.47	0.24	48.98
15	1.00	0.40	60.00
20	1.90	0.59	68.94

1. Advantages

1. Can be used to solve floating dummy conductors
2. Determines the voltage on the dummies, which can be useful in the calculation of crosstalk.
3. Requires only n linear system solves
4. The ground capacitance of the dummies need not be calculated.

Results are shown in Table IV for an example of a single conductor with increased presence of dummy metals. As seen from the table, the new method is computationally very effective for increased number of dummies.

CHAPTER VII

CONCLUSION

In this thesis, an improved method is presented for dynamic force computation which is applicable to both electrostatic and electromagnetic conductors with complex 3D geometries. A simple method based on the principles of fast multipole method (FMM) is explored to effectively recalculate the force using the FMM data structure for the previous time step. It is based on the assumption of uniform charge(current) distributions in a small panel(filament) respectively. The proposed method improves the speed of electrostatic force computation by 15% to 60%, depending on the displacement, with the error less than 3%. Since electromagnetic forces can also be computed by BEM methods, this method can be easily extended. Efficient methods for electrostatic analysis of interconnects in the presence of dummy metal fills were also discussed.

REFERENCES

[1] G. Li and N.R. Aluru, "A Lagrangian approach for electrostatic analysis of deformable conductors," *IEEE J. of Microelectromechanical Systems*, vol. 11, no. 3, pp. 245–254, June 2002.

[2] J.J. Bernstein, W.P. Taylor, J.D. Brazzle, C.J. Corcoran, and G. Kirkos et al., "Electromagnetically actuated mirror arrays for use in 3-D optical switching applications," *IEEE J. of Microelectromechanical Systems*, vol. 13, no. 3, pp. 526–535, June 2004.

[3] S.S. Kuo, M.D. Altman, J.P. Bardhan, B. Tidor, and J.K. White, "Fast methods for simulation of biomolecule electrostatics," in *IEEE/ACM International Conf. on Computer Aided Design, San Jose, CA*, Nov 2002, pp. 466 – 473.

[4] M. Yamaguchi, S. Kawamura, K. Minami, and M. Esashi, "Distributed electrostatic micro actuator," in *IEEE Proc. Micro Electro Mechanical Systems, An Investigation of Micro Structures, Sensors, Actuators, Machines and Systems.*, Feb 1993, pp. 18–23.

[5] S.D. Senturia, N. Azuru, and J. White, "Simulating the behavior of mems devices: computational methods and needs," *IEEE Computational Science and Engineering*, vol. 4, no. 1, pp. 30–43, Jan-March 1997.

[6] J. Wang and J. White, "Fast algorithms for computing electrostatic geometric sensitivities," in *IEEE International Conf. on Simulation of Semiconductor Processes and Devices, Cambridge, MA*, Sept 1997, pp. 121–123.

[7] W. Grobman, M. Thompson, R. Wang, C. Yuan, and R. Tian et al., "Reticle enhancement technology: implications and challenges for physical design," in

IEEE Proc. of Design Automation Conference, Las Vegas, NV, June 2001, pp. 73–78.

[8] B.E. Stine, D.S. Boning, J.E. Chung, L. Camilletti, and F. Kruppa et al., "The physical and electrical effects of metal-fill patterning practices for oxide chemicalmechanical polishing processes," *IEEE Trans. Electron Devices*, vol. 45, no. 3, pp. 665–679, March 1998.

[9] A.A. Appel, "An efficient program for many-body simulation," *SIAM J. on Scientific and Statistical Computing*, vol. 6, no. 1, pp. 85–103, 1985.

[10] J. Barnes and P. Hut, "A hierarchical O(n log n) force calculation algorithm," *Nature*, vol. 324, no. 4, pp. 446–449, Dec 1976.

[11] L. Greengard, *The Rapid Evaluation of Potential Fields in Particle Systems*, Cambridge, MA: MIT Press, 1988.

[12] K. Esselink, "The order of Appel's algorithm," *Information Processing Letters*, vol. 41, no. 3, pp. 141–147, 1992.

[13] L. Greengard and V. Rohklin, "A fast algorithm for particle simulations," *J. of Computational Physics*, vol. 73, no. 2, pp. 325–348, 1987.

[14] K. Nabors and J. White, "Fastcap: a multipole accelerated 3-D capacitance extraction program," *IEEE Trans. Computer- Aided Design, Santaclara, CA*, vol. 10, no. 11, pp. 1447–1459, Nov 1991.

[15] W. Shi, J. Liu, N. Kakani, and T. Yu, "A fast hierarchical algorithm for 3-D capacitance extraction," in *25th ACM/IEEE Proc. of Design Automation Conference, Anaheim, CA*, June 1998, pp. 212–217.

[16] S. Yan, J. Liu, and W. Shi, "Improving boundary element methods for parasitic extraction," in *IEEE Proc. of the ASP-DAC 2003, Kitakyushu, Japan*, Jan 2003, pp. 261–267.

[17] M. Bachtold, M. Emmenegger, J.G. Korvink, and H. Baltes, "An error indicator and automatic adaptive meshing for electrostatic boundary element simulations," *IEEE Trans. Computer Aided Design, San Jose, CA*, vol. 16, no. 12, pp. 1439–1446, Dec 1997.

[18] M. Kamon, M.J. Ttsuk, and J.K. White, "Fasthenry: a multipole-accelerated 3-D inductance extraction program," *IEEE Trans. Microwave Theory Tech.*, vol. 42, no. 9, pp. 1750–1758, Sep 1994.

[19] O. Cueto, F. Charlet, and A. Farcy, "An efficient algorithm for 3d interconnect capacitance extraction considering floating conductors," in *IEEE International Conf. on Simulation of Semiconductor Processes and Devices, Kobe, Japan*, Sept 2002, pp. 107–110.

APPENDIX A

FORCE CALCULATION USING FASTHENRY

A. Magnetostatic Force

The force acting on the filaments can be expressed in the matrix form as

$$F_b = I_b \; dL \; I_b^T \tag{A.1}$$

where I_b is the vector of filament currents, dL is the matrix of gradient of the inductance between the filaments and F_b is the vector of filament forces.

The matrix vector product $(dL \; I_b^T)$ can be computed by Fast Multipole algorithm in $O(b)$ time, where b is the number of filaments.

$$\begin{aligned}(dL \; I_b^T)_i &= -\sum_{\substack{j=1 \\ j\neq i}}^{b} \left(\frac{\mu_0}{4\pi a_i a_j} \int_{V_i} \int_{V_j'} \frac{(l_i \cdot l_j)(r - r')}{\parallel r - r' \parallel^3} dV' dV \right) I_j \\ &= -\frac{1}{a_i} \int_{V_i} C(r) \cdot l_i dV\end{aligned}$$

where

$$C(r) = \frac{\mu_0}{4\pi} \sum_{\substack{j=1 \\ j\neq i}}^{b} \left(\int_{V_j'} \frac{(r - r')}{\parallel r - r' \parallel^3} dV' dV \right) l_j \frac{I_j}{a_j} \tag{A.2}$$

The vector components of $C(r)$ corresponding to the p^{th} component of l_j can be considered as the field vector $E_p(r)$ given by

$$E_p(r) = \frac{\mu_0}{4\pi} \sum_{\substack{j=1 \\ j\neq i}}^{b} \left(\int_{V'_j} (l_j)_p \frac{(r - r')}{\parallel r - r' \parallel^3} dV' dV \right) \frac{I_j}{a_j} \tag{A.3}$$

which is similar to electrostatic field vector with $\frac{I_j}{a_j}(l_j)_p$ interpreted as the charge density due to filament j.

The vector components of $C(r)$ can thus be computed by Fast Multipole methods by computing the gradient of the potential field.

B. Computation by Fast Multipole Method

1. Upward Pass

Compute multipole expansions about the centers of all cubes at all mesh levels, each expansion representing the force coefficient due to particles in the cube. This is the same implementation as that of computing the potential field in Fasthenry.

mulMatUp

Computes the multipole to multipole(mulMulti2Multi) or charge to multipole (mulQ2Multi) matrices that map to a parent's multipole coefficients from its children's multipoles or charges.

mulQ2Multi

Form multipole expansion matrix of the charges at the finest level.

mulMulti2Multi

Translate the multipole expansion matrix of the kid to the parents at coarser mesh levels.

mulUp

Form the multipole coefficient matrix as the product of multipole expansion matrix with the charge vector.

2. Downward Pass

Computes a local expansion about the center of each cube at each mesh level. This local expansion describes the force field due to all particles in the system that are not contained in the current cube, its nearest neighbors, or its second nearest neighbors.

Once the local expansion is obtained for a given cube, it is shifted, to the centers of the cube's children at the next level. Local expansion is obtained for each component of the force coefficient by the gradient of the potential field.

mulMatDown_dL

Sets up local expansion matrices for downward pass by converting the multipole expansion to a local expansion(mulMulti2Local_dir), shifting local expansion of parent to kids(mulLocal2Local_dir) and direct computation of local expansions for distant charges(mulQ2Local_dir) about the center of box and add local expansions together.

mulMulti2Local_dL

Converts the multipole expansions of the each box in the interaction list to local expansions.

mulLocal2Local_dL

Shifts the local expansion of the parent to the children.

mulQ2Local_dL

Sets up local expansion for distant cube charges.

mulDown_dL

Computes the local coefficients by multiplying the local expansions and charges contained in each box

3. Evaluation Pass

Evaluate force coefficient C at the finest level

mulMatEval_fmm

Compute the matrices for evaluating force coefficient from local coefficients (mulLocal2C), multipole coefficients (mulMulti2C) and directly from charges (mulQ2C).

mulLocal2C

Compute matrices to evaluate the local coefficients at each charge position to form force coefficients.

mulMulti2C

Form matrices for computing the force coefficients from multipole coefficients of cubes in the interaction lists.

mulQ2C

Form matrices for computing the force coeffients from charges of cubes in the interaction lists. This is done when the no. of charges is less than the no. of terms in the multipole expansion.

4. Direct Pass

Compute force coefficients C due to near neighbors directly. Implemented in functions mulMatDirect_fmm, mulQ2C

5. Total Force Coefficient C

Add the far field and direct terms together.

VITA

Prabhavathi Koteeswaran was born in Trichy, Tamil Nadu, India in July, 1982. She received her Bachelor of Engineering in electrical and electronics engineering from Anna University, Chennai, India in May 2002. She enrolled in the M.S. program in computer engineering in August 2002 and received her Master of Science in computer engineering in December 2004. Her permanent address in India is: 52, Minor Trustpuram, Kodambakkam, Chennai, India-600094.

The typist for this thesis was Prabhavathi Koteeswaran.